doi.org/10.1002/hlca.202300221

RESEARCH ARTICLE

HELVETICA chimica acta

Selective Recognition of Aromatic Amino Acids by a Molecular Cleft in Water

Joël F. Keller,[a] Michal Valášek,[b] and Marcel Mayor*[a, b, c]

[a] Department of Chemistry, University of Basel, St. Johann's-Ring 19, CH-4056 Basel, Switzerland, e-mail: marcel.mayor@unibas.ch

[b] Institute for Nanotechnology (INT) and Karlsruhe Nano Micro Facility (KNMFi), Karlsruhe Institute of Technology (KIT), Kaiserstr. 12, 76131 Karlsruhe, Germany

[c] Lehn Institute of Functional Materials, School of Chemistry, Sun Yat-Sen University, Guangzhou 510274, P. R. China

Dedicated to Prof. *Roger Alberto* on the occasion of his 65th birthday

The development of water-soluble hosts for the selective recognition of aromatic amino acids is highly desirable and may serve as a tool to facilitate drug discovery and enable fabrication of sensors for point-of-care monitoring in the context of phenylketonuria disease. This paper presents the synthesis and characterization of a water-soluble molecular cleft which is demonstrated to selectively bind aromatic amino acid guests over other amino acids in aqueous medium, favoring L-Trp over L-Phe and L-Tyr by a factor of approximately five. Host/guest-interaction forces were studied by ^{1}H-NMR titrations complemented by fluorescence titrations and isothermal titration calorimetry. The here presented results provide a starting point for future optimizations in our efforts to selectively identify and quantify individual aromatic amino acids in aqueous medium.

Keywords: host-guest systems, amino acids, molecular recognition, receptors, water chemistry.

Introduction

The molecular recognition and distinction of structurally similar individual amino acids in aqueous solution remains a challenging task to this day. A multitude of architectures have been proposed over the years, and the receptors are usually designed to strongly bind amino acid guests with cationic, anionic or nonpolar side chains. For charged sidechains, pillararenes,[1,2] convergent π-systems[3] and calixarenes[4,5] have been employed, the latter also binding nonpolar amino acids,[5,6] in certain cases specifically aromatic amino acids (**aa**$_{ar}$).[7,8] For the recognition of **aa**$_{ar}$, steric constraints such as defined hydrophobic cavity volumes as in the cyclodextrins and cucurbiturils[9–15] and/or additional specific interactions with π-systems in a variety of other architectures[16–19] are used as further selectivity criteria. Selective recognition of **aa**$_{ar}$ ideally relies on three-point binding of the polar ammonium/carboxylate functions in addition to the aromatic side chain, best addressed by utilizing aromatic interactions that may serve as a powerful tool for guest recognition in aqueous medium.[20,21] The most compact and elegant approach to discriminate between the individual **aa**$_{ar}$ should represent the recognition by rationally designed host molecules: simple enough to provide efficient synthetic access and easy derivatization but equipped with the combination of functionality and shape required for selective guest recognition. The challenging task to engineer a host with suitable recognition motifs in the ideal spatial arrangement is further complicated by the constraints and requirements that the aqueous sensing environment imposes on the design. It is

Supporting information for this article is available on the WWW under https://doi.org/10.1002/hlca.202300221

advantageous to maximize the interactions with the aromatic side chains by using a hydrophobic cavity of guest-complementary volume and surface, which minimizes the desolvation penalty of the host surface directly participating in guest encapsulation, and can make use of the hydrophobic effect. At the same time, the host must be sufficiently water-soluble to avoid self-aggregation, thus the periphery must be substituted with polar groups. Additionally, to gain enough binding enthalpy to overcome the high (partial) desolvation energy of the (zwitter)ionic amino acid backbone from water, the exploitation of solvophobic effects is ideally complemented by dipolar/dipolar, H-bonding or ionic interactions in which the host can engage with polar recognition sites. Recent literature suggests that in aqueous medium, it is beneficial for polar substituents on aromatic guests to be solvent-exposed upon binding to the host and thus retain hydrogen-bonding interactions with the surrounding water.[21] This at first glance counterintuitive notion can be explained by the reduced desolvation penalty that the guest must overcome upon binding. To date, there exist only a small number of synthetic architectures that are capable of selectively binding the natural **aa$_{ar}$** (L-Phe, L-Tyr, L-Trp) over the other canonical amino acids in aqueous medium, and the architectures that can additionally favour one of those amino acids, usually Trp, with high specificity over the other ones, can be counted on the fingers on one hand.[10,11,15–17] In 1985, *Rebek et al.* have reported the synthesis of cleft-shaped molecules incorporating π-systems of various sizes, decorated by two equivalents of an imide with the sterically locked Kemp's triacid.[22,23] It was found that the acridine cleft **AC$_{org}$** is able to selectively extract L-Trp, L-Phe and L-Tyrosine *O*-methyl ether in biphasic $H_2O/CHCl_3$ mixtures from the aqueous to the organic layer, an effect that was not observed with any other amino acid. Unfortunately, the binding could not be studied due to the complete insolubility of their host in water. On the other hand, similar hydroxymethyl-extended structures have been used to engineer water-soluble receptors for cyclic adenosine nucleotides with moderate affinity.[24] In this work, we present the synthesis of acridine cleft **AC$_{aq}$**, a hydroxymethyl-extended and water-soluble analogue of **AC$_{org}$** and the studies on amino acid binding and selectivity we performed with it in aqueous medium.

Results and Discussion

Design of the Receptor

In order to quantify the interaction strength between **aa$_{ar}$** and the acridine/Kemp's triacid imide binding site in aqueous medium, we designed and synthesized a water-soluble derivative of **AC$_{org}$**. This was achieved by incorporating a Kemp's triacid derivative with hydroxymethyl groups at the α-position to the carbonyls on the solvent-exposed face of the cleft, resulting in a water-soluble acridine cleft **AC$_{aq}$** (*Figure 1 B*).

The solubilizing groups were integrated into the molecule such that the aromatic amino acid binding domain, which is hypothesized to consist of the acridine π-system, the acridine nitrogen atom and the carboxylic acids,[23] was not altered.

*Synthesis of Acridine Cleft **AC$_{aq}$***

Cleft **AC$_{aq}$** was assembled in 6 steps starting with the synthesis of a threefold benzyloxymethylated derivative of Kemp's triacid as shown in *Scheme 1*, from commercially available cyclohexane-1,3,5-tricarboxylic acid **1** by modified literature procedures.[24]

Trimethyl ester **2** was readily obtained by Fischer esterification in methanol. Threefold enolization with LDA and nucleophilic substitution with an excess of benzyl chloromethyl ether, followed by repeated recrystallization from methanol afforded the pure *cis*,*cis*-triester **3**. Saponification with NaOH in MeOH afforded the aforementioned derivative of Kemp's triacid **4**. To gain access to the protected diimide cleft **6**, **4** was first quantitatively converted to the corresponding internal anhydride by dehydration in *m*-xylene. The bottleneck of the synthesis proved to be the twofold condensation of anhydride **5** with acridine yellow dye. The highest yields were obtained by refluxing both components for 19 h in *m*-xylene (16–23%) or for 3 h in mesitylene (21%), to afford the six-fold benzyl protected cleft **6** after filtration

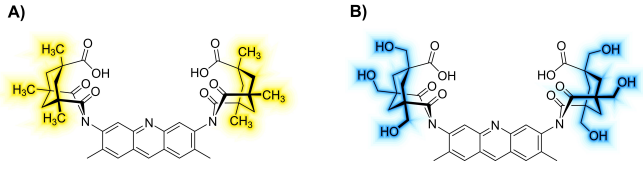

Figure 1. A) Rebek's acridine cleft **AC$_{org}$** with hydrophobic exterior face (yellow), reported to extract **aa$_{ar}$** (L-Phe, L-Tyr, L-Trp) from H_2O to $CHCl_3$. B) The herein presented redesigned water-soluble cleft **AC$_{aq}$** with hydrophilic exterior face (blue).

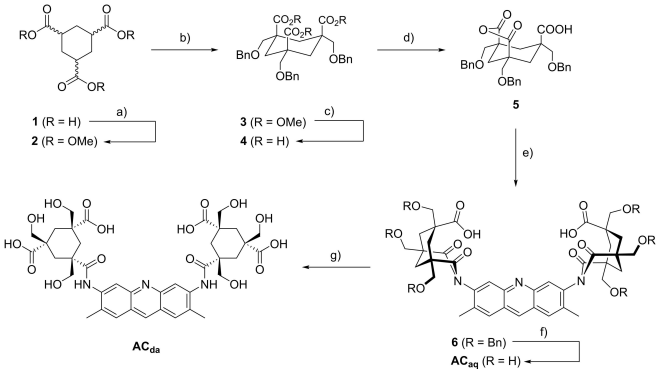

Scheme 1. Reaction Scheme, reagents and conditions for the synthesis of acridine clefts **AC$_{aq}$** and **AC$_{da}$**. a) H_2SO_4, MeOH, reflux, 24 h, 93%, b) 1) LDA, Et_2O, 0 °C, 2 h, 2) benzyl chloromethyl ether, 0 °C -> r.t., 14 h, 31%, c) MeOH, aq. NaOH, reflux, 3 h, 97%, d) *m*-xylene, reflux, 3 h, quant., e) acridine yellow, *m*-xylene, reflux, 3 h, 16%, f) 1) HBr (g), HCO_2H, r.t., 2 h, 2) dilute aq. HCl, r.t., 12 h, quant., g) aq. NaOH, r.t., 12 h, quant.

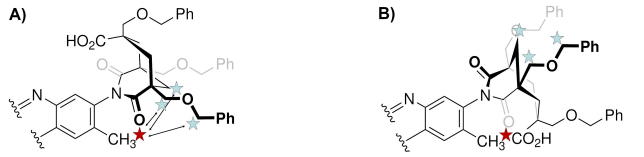

Figure 2. The two possible atropisomeric configurations of the imide arms of acridine cleft **AC$_{aq}$**, carboxylic acid binding site pointing towards A) the interior or B) exterior of the cleft. Configuration A) was confirmed using NOESY NMR, by establishing the NOE contacts between methyl (red) and three sets of $-CH_2$ (blue) protons.

through SiO_2, evaporation of solvents and subsequent trituration with EtOAc and acetone. In order to deprotect the benzyl ethers to the free alcohols, treatment of **6** with HBr (*g*) in neat formic acid gave a mixture of compounds with the scaffold of the desired product **AC$_{aq}$** carrying a varying amount of formyl groups on the six hydroxymethyl groups that were to be liberated. Acid catalyzed hydrolysis of this formyl ester mixture in dilute aqueous HCl solution followed by direct lyophilization of the reaction mixture then afforded the final hexahydroxymethyl acridine cleft **AC$_{aq}$** in quantitative yield and spectroscopically pure. Nevertheless, for ^{1}H-NMR and fluorescence titrations, **AC$_{aq}$** was further purified by HPLC.

*Atropisomerism, Solubility, and Stability of Clefts **AC$_{aq}$** and **AC$_{da}$***

As the rotation of the imide moieties is blocked by the acridine methyl groups,[25] cleft **AC$_{aq}$** has two possible atropisomeric states for each imide site, resulting in three possible isomers, which do not interconvert at room temperature. By establishing the NOE contacts between protons as shown in *Figure 2*, we concluded that only the desired isomer is present, with both carboxylic acids pointing towards the interior of the cleft (*see SI, Figure S24*). Next, we investigated the aqueous solubility and stability of cleft **AC$_{aq}$** in basic and acidic medium. No decomposition of **AC$_{aq}$** was observed in 1 M aq. HCl over the period of multiple days, in stark contrast to what was previously reported for cleft **AC$_{org}$**.[26] We found that albeit **AC$_{aq}$** exhibited good solubility (> 5 mM) in dilute aq. NaOH, clean hydrolysis to the diamide **AC$_{da}$** occurred upon standing overnight. Changing the medium of the highly basic sample of **AC$_{da}$** to 1 M HCl, partial hydrolysis of the amides occurred over the timespan of hours.

^{1}H-NMR Titrations

Cleft **AC$_{aq}$** shows a highly pH-dependent ^{1}H-NMR spectrum in D_2O, with the aromatic signals at the position 4 and 5 of the acridine ring especially affected. The spectra for 1 mM solutions of **AC$_{aq}$** in D_2O or H_2O buffered with 100 mM sodium cacodylate (pH = 5.25), and in 1 M DCl, as well as in D_2O/CD_3CN (1 : 1), buffered with 40 mM AcOD/AcONa (pD = 4.75) and 40 mM deuterated phosphate (pD = 6.6) are compiled in the *Supporting Information*, *Figure S25–S27*. To obtain reliable affinity data from ^{1}H-NMR titrations, it is crucial to keep the pD constant, as well as the total ion strength when titrating with charged guests, which is usually achieved using acid/base buffer solutions as titration medium. The low solubility of zwitterionic aromatic amino acids (in the range of pH = 2–9) in deuterium oxide prompted us to use 1 M DCl in D_2O as titration medium, thereby also approximating constant pD and ion strength throughout the titrations. Cleft **AC$_{aq}$** was titrated with a selection of amino acids (L-Trp, L-Phe, L-Tyr, L-Tyr-*O*-methyl ether, L-His and L-Leu) at constant host concentration of 1 mM, and the results are compiled in *Table 1*.

In all titrations where binding was observed, the acridine C_{aryl}-H signals showed the expected upfield shifts associated with shielding by complexation, the titration with L-Trp and **AC$_{aq}$** is shown as an illustrative example in *Figure 3*. The complete set of titration spectra and details to data fitting[27] for K_a

Table 1. Binding affinities of $\mathbf{AC_{aq}}$ to various amino acid guests and PEA with $[H]_{tot} = 1$ mM, determined by ^{1}H-NMR titrations, in 1 M DCl in D_2O.

Guest	K_a [M^{-1}]
L-Tryptophan	37.1 ± 0.7
L-Phenylalanine	6.7 ± 0.1
L-Tyrosine	7.4 ± 0.1
L-Tyrosine-*O*-methyl ether	6.6 ± 0.1
L-Histidine	– no binding observed –
L -Leucine	– no binding observed –
β-phenylethylamine	2.5 ± 0.1

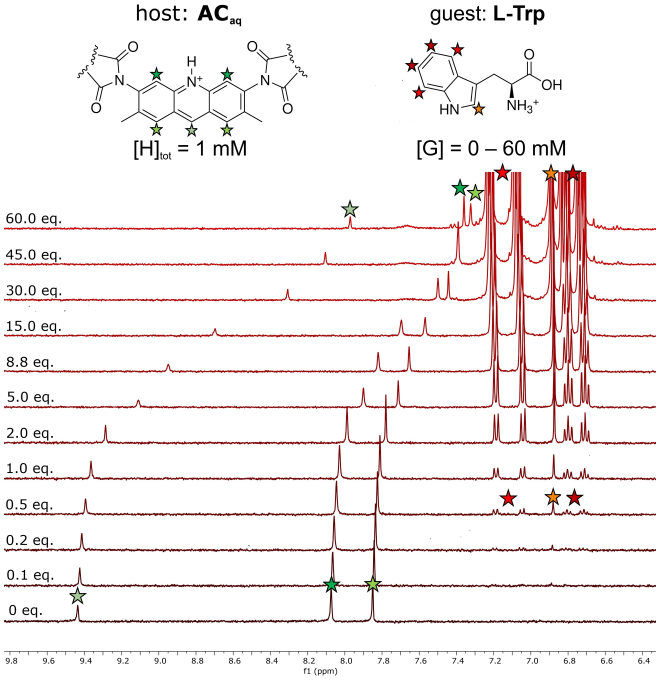

Figure 3. Characteristic upfield evolution of the aromatic proton signals of the acridine moiety of $\mathbf{AC_{aq}}$ in the ^{1}H-NMR titration with 0–60 eq. **L-Trp** upon guest complexation, in 1 M DCl in D_2O at pH = 0.

determination can be found in the *Experimental Section* and *Supporting Information*, *Figures S36–S56* and *Tables S1–S7*. Cleft $\mathbf{AC_{aq}}$ was found to weakly associate with the aromatic amino acids, favoring L-Trp over L-Phe, L-Tyr and L-Tyr-*O*-methyl ether by a factor of 5–6, and bound the latter three with very similar affinities. No binding was observed to L-His, which can be attributed to electrostatic repulsion between the positively charged L-His side chain and the monocationic acridine cleft under the titration conditions. L-Leu also did not show any affinity to $\mathbf{AC_{aq}}$, corroborating the importance of aromatic interactions to the binding energy. The binding domain thus retains its selectivity for aromatic amino acids also in aqueous environment. To gain insight in the contribution of the amino acid carboxylate function to binding and on the grounds of the published excellent binding to $\mathbf{AC_{org}}$ in $CHCl_3$,[28] β-phenylethylamine (PEA) was investigated as guest. Initial promising results in unbuffered CD_3CN/D_2O (1:1) mixture reproduced the upfield shift of acridine protons 4 and 5 between 0 and 0.5 eq. of guest, followed by downfield shift exceeding 0.5 eq., as observed for $\mathbf{AC_{org}}$ in $CHCl_3$ (see *SI, Figure S48*). However, it became clear that these shifts merely represent different protonation states of the receptor caused by the basic guest when performing the titration in CD_3CN/D_2O (1:1) buffered at pD = 4.75 (AcONa/AcOD, 30 mM and 100 mM) and at pD = 6.6 (deuterated phosphate buffer). At sufficient buffer capacity (100 mM), no shift is observed up to 4.6 eq. guest, indicating a $K_a < 1$ (see *SI, Figures S49–S51).* A titration with PEA and $\mathbf{AC_{aq}}$ in 1 M DCl/D_2O was carried out, resulting in improvement of binding (K_a = 2.5 M^{-1}, see *Table 1* and *SI, Figures S46–S47 and Table S5*) as observed with L-Phe, but the absence of the carboxylate function results in approximately threefold lower affinity when comparing to L-Phe under identical conditions, indicating involvement of the carboxylate group of $\mathbf{aa_{ar}}$ in binding. The serendipitously obtained diamide-tetraacid $\mathbf{AC_{da}}$ was also probed for affinity with L-Phe in D_2O/sodium cacodylate buffer (100 mM, pD = 5.25), resulting in a K_a of 10.1 M^{-1} (see *SI, Figures S52–S53 and Table S6*), which is comparable to the result obtained for the binding of L-Phe to $\mathbf{AC_{aq}}$ (in 1 M DCl/D_2O), but tenfold higher than when titrating the imide $\mathbf{AC_{aq}}$ under identical conditions with L-Phe (K_a = 1.3 M^{-1}, see *SI*, Figures *S54–S55* and *Table S7*). Unfortunately, the instability of cleft $\mathbf{AC_{da}}$ in 1 M aq. HCl prevented the titration under these conditions. Nevertheless, these results indicate that the reduced range of motion of the carboxylate binding sites (constrained by the hindered rotation about the imide-C–N-axis in $\mathbf{AC_{aq}}$) does not necessarily contribute to stronger affinity to aromatic amino acids in aqueous medium, as it was observed for $\mathbf{AC_{org}}$ in $CHCl_3/H_2O$ biphasic extraction experiments.[23] A notable peculiarity associated with the titration of L-Trp was a color change from yellow to orange over the addition of the first few equivalents of guest, a trait that was not observed with any other amino acid.

Fluorescence Quenching Titrations

Like the parent compound acridine yellow, the derivative **AC$_{aq}$** is fluorescent and emits blue light with λ_{em} = 502 nm (see *SI*, *Figure S35*) with a large Stokes shift of 137 nm, limiting inner filter effects to a minimum. All guests that showed affinity to **AC$_{aq}$** in ^{1}H-NMR titrations also gradually quenched the host fluorescence with increasing guest concentration in 1 M aq. HCl at pH = 0 and in aqueous sodium formate buffer at pH = 3.9, with L-Trp being most efficient in this regard, as illustrated in *Figure 4*. Fluorescence quenching titrations of **AC$_{aq}$** with excitation at λ_{ex} = 347 nm in aqueous sodium formate buffer (100 mM at pH = 3.9) with L-Trp and L-Phe indeed gave asymptotic quenching series (see *SI*, *Figures S56–S61* and *Tables S8–S10*). Unfortunately, we found that the fluorescence lifetime of **AC$_{aq}$** was reduced in the presence of L-Trp (see *SI*, *Figures S62–S65*, *Table S11*), indicating that the reduction of emission observed in the fluorescence quenching assays stems at least partially from a dynamic quenching mechanism that does not originate from static host/guest complex formation, but simply from statistical encounter and proximity of the two components in solution. Since the exact quenching mechanisms remain unexplored, exact K_a values could not be determined. Fitting the fluorescence titration data to a one-to-one binding model resulted in K_a values in *Table 2*, which overestimate binding because quenching is partially mediated by a dynamic mechanism. Nevertheless, this result is qualitatively in line with the results obtained from ^{1}H-NMR titrations. Fluorescence quenching titration was also performed with the guest L-Tyr-*O*-methyl ether, but upon irradiation with λ_{ex} = 347 nm, unexpected degradation of **AC$_{aq}$** to several breakdown products was observed (by ESI-ToF) and no binding data could be obtained for this guest. Titration with L-Phe gave a value of 41.6 M^{-1}, uncorrected for dynamic quenching. We did not determine the experimental lifetime reduction for L-Phe as quencher/guest but assuming a similar quenching situation as for L-Trp, the obtained value is qualitatively in line with ^{1}H-NMR experiments.

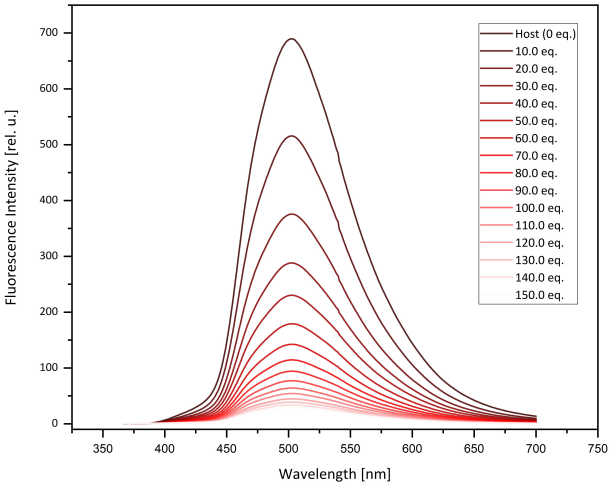

Figure 4. Evolution of the fluorescence emission intensity signal of **AC$_{aq}$** at λ_{em} = 502 nm in the fluorescence quenching titration with 0–150.0 equiv. **L-Trp**, in aq. sodium formate buffer (100 mM) at pH = 3.9.

Table 2. Binding affinities of **AC$_{aq}$** to L-Trp and L-Phe with $[H]_{tot}$ = 0.15 mM, either measured in 1 M aq. HCl (pH = 0) or in 100 mM sodium formate buffer (pH = 3.9), determined by fluorescence quenching titrations.

Guest	pH	K_a [M^{-1}][a]
L-Tryptophan	0	90.4 ± 2.8
L-Tryptophan	3.9	110.7 ± 3.9
L-Phenylalanine	3.9	41.6 ± 1.4

[a] experimental fit, uncorrected for dynamic quenching

Isothermal Titration Calorimetry

To complement the results obtained by ^{1}H-NMR and fluorescence quenching titrations, the binding of L-Trp to cleft **AC$_{aq}$** was further studied by isothermal titration calorimetry (ITC) in 0.1 M aq. HCl solution (pH = 1) and *Certipur*® buffer (citric acid, NaOH, HCl, pH = 2), (see *SI, Figures S66–S79*). Although the low solubility of L-Trp in acidic aqueous solution limited the experimentally feasible maximum of *Wiseman's* c-value[29] with our experimental setup to the value that was also employed in ^{1}H-NMR titrations (c = 0.037–0.074), we were able to obtain K_a values that closely match the results obtained in the NMR experiments by fixing the stoichiometry of binding to a 1:1 host/guest system (N = 1).[30] The thermodynamic signature of binding (favorable enthalpy change, accompanied by an unfavorable entropic term) indicates that host-guest association could be driven by the nonclassical hydrophobic effect as originally proposed by *Diederich* et al.,[31] although conclusions drawn from the shallow binding isotherms regarding △H and △S must be enjoyed with caution. The small ratio between the enthalpic response of the binding event (e.g. *SI, Figures S68–S71*) and the dilution heat of injection at a given guest concentration (e.g. *SI, Figures S66 and S67*), combined with the low c-value and the low solubility limit of the guest made

titration to a sufficiently high [guest]/K_d value i.e. to sufficient flattening of the hyperbolic curve impossible.[32] This makes the host/guest combination suboptimal for the extraction of △H and △S from ITC analysis. However, all titration curves showed the expected non-sigmoidal shape for $c \ll 1$[29,32] and produced small but consistent enthalpic responses at specific molar ratios X_i of guest/host. All ITC titrations gave good agreement with ^{1}H-NMR experiments (K_a difference of factor 1.00–1.21), as shown in *Table 3*, entries with pH = 1, 298 K. Attempts to titrate **AC$_{aq}$** with L-Trp at lower c-values generally led to a too high signal-to-noise ratio, which made adequate curve fitting and extraction of K_a values impossible.

Conclusions

An efficient and scalable synthesis of water-soluble acridine cleft **AC$_{aq}$** composed of hydroxymethylated Kemp's triacid and acridine yellow is presented. Cleft **AC$_{aq}$** was fully characterized (^{1}H-NMR, ^{13}C NMR, and HR-MS-ESI) and titrated (^{1}H-NMR, fluorescence quenching and ITC) for affinity with several amino acids and the truncated structural analog PEA. In ^{1}H-NMR titration experiments, weak complex formation, dependent on the size of the side chain aromatic surface and pH (ca. 1–70 M^{-1}), was observed exclusively for aromatic amino acids and to a lesser extent, for PEA. The electron density of the aromatic side chain (L-Phe vs. L-Tyr vs. L-Tyr-O-methyl ether) did not seem to modulate K_a significantly. No affinity was observed for non-aromatic amino acids, indicating that the binding site retains its selectivity for aromatic amino acids in water. A decrease in affinity could be observed at pH = 5.25 for L-Phe compared to pD = 0. Absence of the amino acid carboxylate function in PEA also resulted in diminished binding, and the pH/pD dependence could additionally be corroborated for PEA at pD = 0, pD = 4.75 and pD = 6.6. In contrast, the tetraacid-diamide **AC$_{da}$** was found to bind L-Phe in the zwitterionic state at pH = 5.25 with eight-fold higher affinity than **AC$_{aq}$**, however, the instability of **AC$_{da}$** under acidic conditions prevented further comparative study. L-Trp and L-Phe were found to quench the fluorescence of **AC$_{aq}$** in fluorescence titrations. A lifetime reduction of the host fluorescence was observed upon guest addition, suggesting a partially dynamic contribution to quenching, limiting the validity of the extracted K_a values from these assays. Nevertheless, the results were qualitatively in line with the ^{1}H-NMR titration data. ITC titrations of L-Trp at pH = 1 and pH = 2 into **AC$_{aq}$** further provided good agreement with the value obtained from ^{1}H-NMR experiments. The ability of the herein presented receptor **AC$_{aq}$** to selectively bind aromatic amino acids in aqueous medium has been reported before but is a rare quality. Although the affinities cannot match those of some already published systems,[10,11,13,15–17] the achievable selectivity of **AC$_{aq}$** or easily accessible future derivatives thereof for **aa$_{ar}$** over related biogenic amines and/or carboxylates, as well as electron-rich, unfunctionalized aromatics is expected to be high, due to multipoint-binding of **aa$_{ar}$** in aqueous environment.

Table 3. Binding affinities, enthalpy and entropy of binding of **AC$_{aq}$** ($[H]_{tot}$ = 1 mM) to L-Trp, measured in either 0.1 M aq. HCl (pH = 1) or in *Certipur*® citrate buffer (pH = 2), determined by ITC.

pH [ ]	*T* [K]	X_i[c] [ ]	K_a [M^{-1}]	ΔH [kJmol^{-1}]	−TΔS [kJmol^{-1}]
1	298[a]	9.5	37.2 ± 2.7	-27.3 ± 1.6	18.3
		19	43.7 ± 2.7	-23.4 ± 1.0	14.1
	293[b]	9.5	43.3 ± 1.3	-27.4 ± 0.7	18.2
		19	48.8 ± 2.8	-25.6 ± 1.0	16.1
2	293[b]	5.7	35.1 ± 1.0	-37.1 ± 0.9	28.5
		11.3	49.3 ± 0.6	-32.3 ± 0.3	22.8
	288[b]	5.7	53.8 ± 2.0	-30.1 ± 0.9	20.5
		12.3	68.5 ± 0.9	-24.5 ± 0.2	14.4

[a] measured with a spacing of 150 s between injections
[b] measured with a spacing of 300 s between injections [c] X_i (guest/host) refers to the molar ratio of guest to host at the endpoint of titration. The statistical errors refer to the reliability of the non-linear regression calculations of single titrations.

Experimental Section

The synthesis of literature known compounds **2**–**5**,[24] ^{1}H-NMR, ^{13}C NMR, HRMS UV/Vis and fluorescence spectra, titration data (^{1}H-NMR, fluorescence, ITC), as well as lifetime measurements can be found in the Supporting Information.

General Remarks

Synthesis and Characterization of Compounds

Deuterated solvents were obtained from Cambridge Isotope Laboratories, Inc. (Andover, MA, USA). All commercially available compounds were purchased from SigmaAldrich (Switzerland), Acros, Apollo Scien-

tific, Alfa Aesar and Fluorochem (United Kingdom). Column chromatography was performed on silica gel P60 (40–63 μm) from SilicycleTM, the solvents were technical grade. TLC was performed with silica gel 60 F254 aluminium plates purchased from Merck. Analytics and instruments: NMR experiments were performed on Bruker Avance III NMR spectrometers operating at 400, 500 or 600 (cryoprobe) MHz proton frequencies. The instruments were equipped with a direct-observe 5 mm BBFO smart probe (400 MHz), or an indirect-detection 5 mm BBI probe (500 MHz), or a five-channel cryogenic 5 mm QCI probe (600 MHz). All probes were equipped with actively shielded z-gradients (10 A). The chemical shifts are reported in ppm relative to tetramethylsilane or referenced to residual solvent peak and the *J* values are given in Hz (±0.1 Hz). Standard Bruker pulse sequences were used, and the data was processed on Topspin 3.2 (Bruker) using twofold zero-filling in the indirect dimension. UV-Vis absorption spectra were recorded at 20 °C on a Jasco V-770 Spectrophotometer. Lifetime decay measurements were performed on a LifeSpec II setup (Edinburgh Instruments), using time-correlated single photon counting technique (TCSPC), a picosecond pulsed diode laser (320 nm, ca. 75.5 ps pulse width) was used for excitation. High-pressure liquid chromatography (HPLC) was performed on a Shimadzu Prominence System. For high resolution mass spectrometry (HRMS) a HR-ESI-ToF-MS measurement on a maXisTM 4G instrument from Bruker was performed. When indicated and to obtain anhydrous solvents, *N,N*-diisopropylamine and Et_2O were distilled from sodium and benzophenone, and *m*-xylene was refluxed and distilled from sodium hydride. Anhydrous hydrogen bromide gas for debenzylation was synthesized *in situ* by dropwise addition of conc. H_2SO_4 to stirred solid KBr, and conducting the resulting gas directly into the reaction mixture through a Tygon® tube of sufficient length, to avoid contamination of the reaction mixture with elemental bromine. **^{1}H-NMR titrations, binding isotherm extraction & fitting, calculation of K_a values**: In order to keep the pD and ion strength constant, ^{1}H-NMR titration experiments were performed in 1 M DCl in D_2O (pD = 0), in sodium cacodylate buffer (100 or 300 mM, + 500 mM NaCl, pH = 5.25) measured with water suppression, in D_2O buffered with AcOD/AcONa (pD = 4.75) or in D_2O buffered with deuterated phosphate buffer (pD = 6.6). The spectra were referenced to HDO (4.79 ppm) in titrations in D_2O, and in titrations with cacodylate buffer in 95% H_2O, referenced to the methyl signal of cacodylate (1.89 ppm). The host (**AC_{aq}** or **AC_{da}**) concentration was always 1 mM, and was kept constant during the titration, whereas the concentration of the amino acid guest was varied and titrated until its solubility limit was reached or until only negligible chemical shift change occurred upon further addition of guest. The experiments were performed at room temperature. Displayed in the ^{1}H-NMR titration graphs (Supporting Information) are the relevant portions of the aromatic region of host (**AC_{aq}**), from which the relative chemical shift changes $\Delta\delta$ for the three distinct acridine aromatic C–H signals over the course of the titrations were extracted. K_a values were obtained by multiparametric fitting of the evolution of $\Delta\delta$ for the three acridine C–H signals by using the publicly available Matlab script written by P. Thordarson[20] for ^{1}H-NMR 1:1 binding. **Fluorescence quenching titrations**: Fluorescence quenching titrations were performed at 20 °C on a Jasco FP-8600 Spectrofluorometer. All fluorescence quenching titrations were carried out at a $[H]_{tot} = 0.15$ mM, with OD = 0.48 at 365 nm, which was kept constant throughout the measurement series. Titrations at pH = 3.9 were carried out in aqueous sodium formate buffer (100 mM), and titrations at pH = 0 in 1 M aq. HCl. The excitation wavelength was $\lambda_{ex} = 347$ nm, and the fluorescence intensity at the emission maximum $\lambda_{em} = 502$ nm was recorded. Samples were mixed and equilibrated for 15 min after guest solution addition, before a datapoint was recorded. **Isothermal Titration Calorimetry**: All isothermal titration calorimetry (ITC) experiments were carried out on a MicroCal PEAQ-ITC instrument from Malvern Panalytical. All titrations were carried out in 0.1 M HCl at pH = 1, or in *Certipur*® buffer (citric acid, NaOH, HCl) at pH = 2 with a host **AC_{aq}** concentration of 1 mM in the measurement cell (representing a c-value identical to ^{1}H-NMR titrations) and a guest L-Trp concentration of 50 mM or 100 mM (pH = 1) or 30 mM, 60 mM or 65 mM (pH = 2) in the injection syringe. In each titration, an initial injection of 0.4 μL was followed by 18 injections of 2 μL to the measurement cell. The cell temperature was kept at either 288 K, 293 K or 298 K. Reference measurements of injection heat and titrations were performed against a reference power of 50 μW (pH = 1, 293 K and 298 K), 42 μW (pH = 2, 288 K) or 30 μW (pH = 2, 293 K). The spacing between individual injections was either 150 s or 300 s. Heat changes were recorded after each addition. Dilution (injection) heats were subtracted from the titration data prior to curve fitting. Every titration was done at least two times. The first smaller injection (0.4 μL) was

discarded from each data set to remove the effect of guest diffusion across the syringe tip during the equilibration process. Titration curves were fitted using PEAQ-ITC Analysis software supplied by Micro-Cal with the one-set-of-sites binding model and fixing the binding stoichiometric parameter N to 1 for our low affinity system ($c \ll 1$).

(1*S*,5*R*,7*r*)-1,5,7-Tris[(benzyloxy)methyl]-*N*-(2,7-dimethyl-6-{(1′*R*,5′*S*,7′*s*)-',5′,7′-tris[(benzyloxy)methyl]-7′-carboxy-2′,4′-dioxo-3′-azabicyclo[3.3.1]nonan-3′-yl}acridin-3-yl)-2,4-dioxo-3-azabicyclo[3.3.1]nonane-7-carboxylic acid (6)

To obtain acridine yellow free-base, commercial acridine yellow·HCl (1.02 g) was suspended in MeOH (500 mL), and aq. 3 M NaOH (250 mL) was added. The mixture was stirred for 10 min at room temperature, and filtered by suction. The methanol was carefully removed to a residual volume of 150 mL under reduced pressure, resulting in precipitation of the free-base from the residual aqueous layer. The free base was filtered by suction, and dried in high vacuum at 70 °C for 1 h to give a yellow-brownish powder (570 mg). 250 mg of the brownish material was suspended in *m*-xylene (70 mL) and heated to reflux for 10 min. The suspension was cooled in an ice bath for several minutes, until all solids had precipitated. The suspension was filtered, and the solids dried in high vacuum, to give acridine yellow free-base as a pale yellow solid (220 mg). **5** (660 mg, 1.14 mmol, 2.00 eq.) was dissolved in *m*-xylene (100 mL) in a 250 mL three-necked round-bottom flask equipped with a Dean-Stark-apparatus and reflux condenser. Acridine yellow free-base (135 mg, 0.569 mmol, 1.00 eq.) was added in one portion, and the reaction mixture was stirred for 20 h at 115 °C, subsequently refluxed for 18 h, and was allowed to cool to room temperature. The solvent was evaporated *in vacuo* at 55 °C, to give the crude material as a dark brown semisolid. The crude material was filtered through SiO_2, eluting with EtOAc/MeOH (90:10), and the solvent was evaporated. The residue was suspended in EtOAc/acetone (3:1, 80 mL), and heated to reflux for several minutes. Upon cooling to room temperature, a colorless precipitate formed, which was filtered, and the solids washed with acetone (2×4 mL), to give **6** (*Figure 5*) as an off-white solid (120 mg, 0.091 mmol, 16 %).

^{1}H-NMR (600 MHz, DMSO-d_6) $\delta = 13.12$ (*s*, 2H, -COOH), 8.93 (s, 1H, H–C(8)), 8.11 (*s*, 2H, H–C(4)), 8.00 (*s*, 2H, H–C(7)), 7.38–7.26 (*m*, 30H, H-C_{aryl}), 4.51 (*s*, 8H, H–C(15)), 4.49 (*s*, 4H, H–C(16)), 3.91 (*d*, $J = 8.9$ Hz, 4H, H–C(13)), 3.45 (*s*, 4H, H–C(14)), 3.42 (*d*, $J = 9.1$ Hz, 4H, H–C(13)), 2.84 (*d*, $J = 13.2$ Hz, 2H, H–C(9)), 2.44 (*d*, $J = 13.7$ Hz, 4H, H–C(11)), 2.07 (*s*, 6H, H–C(1)), 1.72 (*d*, $J = 13.4$ Hz, 2H, H–C(9)), 1.65 (*d*, $J = 13.9$ Hz, 4H, H–C(11)) ppm. **^{13}C NMR** (101 MHz, DMSO-d_6) $\delta = 175.35$ (C17), 173.96 (C18), 147.34 (C5), 138.30 (C_{ar}), 138.26 (C3), 138.10 (C_{ar}), 133.78 (C8), 133.73 (C2), 128.52 (C4), 128.27 (C_{ar}), 128.19 (C_{ar}), 127.95 (C7), 127.48 (C_{ar}), 127.41 (C_{ar}), 127.29 (C_{ar}), 127.20 (C_{ar}), 126.10 (C6), 78.38 (C14), 74.70 (C13), 72.66 (C15), 72.37 (C16), 45.69 (C12), 44.42 (C10), 33.81 (C11), 33.14 (C9), 17.37 (C1) ppm. **HR-MS**: (ESI-ToF, +): m/z = $[M+H]^+$ Calcd. For $C_{81}H_{80}N_3O_{14}$: 1318.5635; Found 1318.5623.

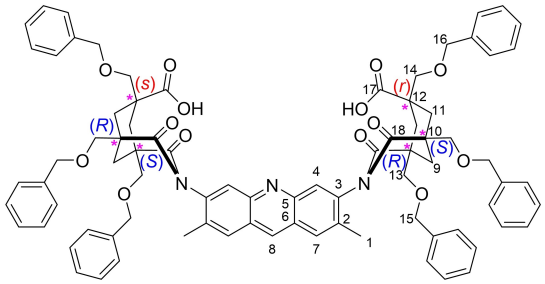

Figure 5. Chemical structure of precursor **6** comprising carbon numbering for NMR assignment.

N-{6-[7′-Carboxy-(1′*R*,5′*S*,7′*s*)-tris(hydroxymethyl)-2′,4′-dioxo-3′-azabicyclo[3.3.1]nonan-3′-yl]-2,7-dimethylacridin-3-yl}-(1*S*,5*R*,7*r*)-tris(hydroxymethyl)-2,4-dioxo-3-azabicyclo[3.3.1]nonane-7-carboxylic acid (AC_{aq})

Compound **6** (402 mg, 0.305 mmol, 1.00 eq.) was dissolved in formic acid (100 mL), and HBr (*g*) was bubbled through the solution for 15 min at room temperature, and stirring was continued. The reaction was monitored with LC–MS-ESI and as soon as the substrate was fully debenzylated and converted to the six-fold formic acid ester (946.3 m/z, $M+1$) after 2.5 h of stirring time, a stream of argon (*g*) was passed through the solution for 10 min and the solvent was evaporated *in vacuo*. To the brown oily residue, iPrOH (80 mL) was added, followed by cyclohexane (220 mL). The yellow precipitate was allowed to settle and the supernatant was decanted, to a residual suspension volume of approx. 15 mL. This was centrifuged, the supernatant discarded, and the pellet washed with cyclohexane (1×3 mL). The yellow solid was dried *in vacuo*, redissolved in 0.05 M

aq. HCl (53 mL), and stirred at room temperature for 18 h. The colorless polymeric precipitate was filtered off by gravity through a cotton filter, and the filtrate was lyophilized, to provide **AC_{aq}** (*Figure 6*) as a yellow fluffy solid (237 mg, 0.304 mmol, quant.) For ^{1}H-NMR titrations, UV-Vis measurements and fluorescence emission quenching titrations, the compound was further purified by HPLC using the following conditions: Isocratic flow with acetonitrile/water (15:85) + 1% formic acid. The retention time is 5 min on a Reprosil C18 analytical column (5 μm mesh, 250 mm length and 4.6 mm internal diameter, flow: 1.5 mL/min), and on a Reprosil C18 preparative column (10 μm mesh, 250 mm length, 30 mm internal diameter) with a flow of 31.9 mL/min, the retention time is 7 min.

^{1}H-NMR (400 MHz, D_2O/CD_3CN (1:1), referenced to HDO at 4.79 ppm) δ = 10.21 (*s*, 1H), 8.90 (*s*, 2H), 8.73 (*s*, 2H), 4.56 (*d*, *J* = 11.4 Hz, 4H), 4.13 (*s*, 4H), 4.05 (*d*, *J* = 11.4 Hz, 4H), 3.29 (*d*, *J* = 13.4 Hz, 2H), 3.01 (*d*, *J* = 14.0 Hz, 4H), 2.82 (*s*, 6H), 2.14 (*d*, *J* = 13.5 Hz, 2H), 2.07 (*d*, *J* = 14.2 Hz, 4H) ppm. **^{13}C NMR** (101 MHz, D_2O/CD_3CN (1:1), referenced to HDO at 4.79 ppm) δ = 178.71, 177.08, 147.35, 144.91, 140.41, 138.01, 131.35, 127.56, 121.20, 71.50, 67.21, 48.23, 46.82, 34.55, 33.28, 18.14 ppm. **HR-MS**: (ESI-ToF, +): m/z = $[M+H]^+$ Calcd. For $C_{39}H_{44}N_3O_{14}$: 778.2818; Found 778.2807.

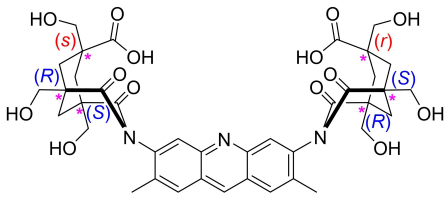

Figure 6. Chemical structure of **AC_{aq}** comprising stereodescriptors.

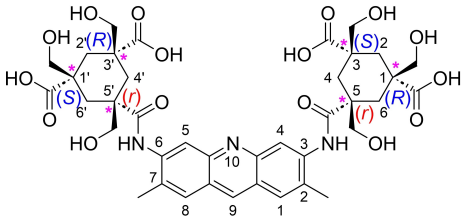

Figure 7. Chemical structure of **AC_{da}** comprising IUPAC numbering of the subunits.

(1*R*,1′*S*,3*S*,3′*R*,5*r*,5′*r*)-5,5′-[*N*,*N*-(2,7-Dimethylacridine-3,6-diyl)dicarbamoyl]bis[1,3,5-tris(hydroxymethyl)cyclohexane-1,3-dicarboxylic acid] (AC_{da})

To a solution of **AC_{aq}** (1 mg) in D_2O (0.6 mL) in a high-throughput glass NMR tube was added 1 drop of 1 M aq. NaOH solution and the solution was left to stand for 14 h, to provide the tetraacid-diamide **AC_{da}**. (*Figure 7*).

^{1}H-NMR (400 MHz, D_2O) δ = 8.85 (*s*, 1H), 8.35 (*s*, 2H), 8.17 (*s*, 2H), 7.89 (*s*, 2H), 3.61 (*s*, 4H), 3.51 (*s*, 8H), 2.64 (*d*, *J* = 15.0 Hz, 4H), 2.42 (*s*, 6H), 1.81 (*s*, 4H), 1.47 (*d*, *J* = 14.9 Hz, 2H), 1.33 (*d*, *J* = 15.2 Hz, 4H) ppm. **^{13}C NMR** (151 MHz, D_2O) δ = 183.61, 178.34, 170.99, 160.25, 141.16 (extracted from HMBC), 138.55 (extracted from HMQC), 133.30, 128.80, 124.51, 71.26, 70.16, 48.20, 47.48, 32.63, 31.14, 17.65 ppm. **HR-MS**: (ESI-ToF, +): m/z = $[M+H]^+$ Calcd. For $C_{39}H_{48}N_3O_{16}$: 814.3029; Found 814.3016.

Author Contribution Statement

J.F.K. performed chemical synthesis and characterization of all compounds, performed ^{1}H-NMR and fluorescence titrations and corresponding data analysis and isotherm fitting, lifetime measurements, and wrote the manuscript. M.V. performed ITC titrations and corresponding isotherm fitting. M.M. supervised the work and wrote the manuscript. All authors commented on the manuscript.

Acknowledgements

The authors acknowledge generous support by the Swiss National Science Foundation (SNF Grant no. 200020-207744) and by the NCCR "Molecular Systems Engineering" (SNF Grant no. 51NF40-141825). M.M. acknowledges support from the 111 project (Grant No. 90002-18011002). Open Access funding provided by Universität Basel. M.V. and M.M. gratefully acknowledge financial support from the Helmholtz Association via the program Materials Systems Engineering (MSE). Open Access funding provided by Universität Basel.

Conflict of Interest

The authors declare no conflict of interest.

Data Availability Statement

The data that support the findings of this study are available in the supplementary material of this article.

References

[1] M. Bojtár, A. Paudics, D. Hessz, M. Kubinyi, I. Bitter, 'Amino acid recognition by fine tuning the association constants: tailored naphthalimides in pillar[5]arene-based indicator displacement assays', *RSC Adv.* **2016**, *6*, 86269–86275.

[2] Q. Duan, W. Zhao, K. Lu, 'Synthesis of a water-soluble pillar[6]arene dodecaamine and its selective binding of acidic amino acids in water', *Tetrahedron Lett.* **2017**, *58*, 4403–4406.

[3] T. Schrader, G. Bitan, F.-G. Klärner, 'Molecular tweezers for lysine and arginine - powerful inhibitors of pathologic protein aggregation', *Chem. Commun.* **2016**, *52*, 11318–11334.

[4] N. Douteau-Guével, A. W. Coleman, J.-P. Morel, N. Morel-Desrosiers, 'Complexation of the basic amino acids lysine and arginine by three sulfonatocalix[n]arenes (n = 4, 6 and 8) in water: microcalorimetric determination of the Gibbs energies, enthalpies and entropies of complexation', *J. Chem. Soc. Perkin Trans. 2* **1999**, 629–634.

[5] F. Perret, A. N. Lazar, A. W. Coleman, 'Biochemistry of the para-sulfonato-calix[n]arenes', *Chem. Commun.* **2006**, 2425.

[6] W. Zielenkiewicz, A. Marcinowicz, S. Cherenok, V. I. Kalchenko, J. Poznański, 'Phosphorylated Calixarenes as Receptors of L-Amino Acids and Dipeptides: Calorimetric Determination of Gibbs Energy, Enthalpy and Entropy of Complexation', *Supramol. Chem.* **2006**, *18*, 167–176.

[7] F. Sansone, S. Barboso, A. Casnati, D. Sciotto, R. Ungaro, 'A new chiral rigid cone water soluble peptidocalix[4]arene and its inclusion complexes with α-amino acids and aromatic ammonium cations', *Tetrahedron Lett.* **1999**, *40*, 4741–4744.

[8] M. Torvinen, R. Neitola, F. Sansone, L. Baldini, R. Ungaro, A. Casnati, P. Vainiotalo, E. Kalenius, 'Glucosylthioureidocalix-[4]arenes: Synthesis, conformations and gas phase recognition of amino acids', *Org. Biomol. Chem.* **2010**, *8*, 906–915.

[9] M. A. Gamal-Eldin, D. H. Macartney, 'Selective molecular recognition of methylated lysines and arginines by cucurbit[6]uril and cucurbit[7]uril in aqueous solution', *Org. Biomol. Chem.* **2013**, *11*, 488–495.

[10] M. E. Bush, N. D. Bouley, A. R. Urbach, 'Charge-Mediated Recognition of N-Terminal Tryptophan in Aqueous Solution by a Synthetic Host', *J. Am. Chem. Soc.* **2005**, *127*, 14511–14517.

[11] J. Lagona, B. D. Wagner, L. Isaacs, 'Molecular-Recognition Properties of a Water-Soluble Cucurbit[6]uril Analogue', *J. Org. Chem.* **2006**, *71*, 1181–1190.

[12] Z.-Z. Gao, J.-L. Kan, L.-X. Chen, D. Bai, H.-Y. Wang, Z. Tao, X. Xiao, 'Binding and Selectivity of Essential Amino Acid Guests to the Inverted Cucurbit[7]uril Host', *ACS Omega* **2017**, *2*, 5633–5640.

[13] J. W. Lee, H. H. L. Lee, Y. H. Ko, K. Kim, H. I. Kim, 'Deciphering the Specific High-Affinity Binding of Cucurbit[7]uril to Amino Acids in Water', *J. Phys. Chem. B* **2015**, *119*, 4628–4636.

[14] H.-J. Buschmann, E. Schollmeyer, L. Mutihac, 'The formation of amino acid and dipeptide complexes with α-cyclodextrin and cucurbit[6]uril in aqueous solutions studied by titration calorimetry', *Thermochim. Acta* **2003**, *399*, 203–208.

[15] P. Stepniak, B. Lainer, K. Chmurski, J. Jurczak, 'The effect of urea moiety in amino acid binding by β-cyclodextrin derivatives: A 1000-fold increase in efficacy comparing to native β-cyclodextrin', *Carbohydr. Polym.* **2017**, *164*, 233–241.

[16] L. Cheng, H. Zhang, Y. Dong, Y. Zhao, Y. Yu, L. Cao, 'Tetraphenylethene-based tetracationic cyclophanes and their selective recognition for amino acids and adenosine derivatives in water', *Chem. Commun.* **2019**, *55*, 2372–2375.

[17] T. T. Goodnow, M. V. Reddington, J. F. Stoddart, A. E. Kaifer, 'Cyclobis(paraquat-p-phenylene): a novel synthetic receptor for amino acids with electron-rich aromatic moieties', *J. Am. Chem. Soc.* **1991**, *113*, 4335–4337.

[18] A. Dalla Cort, P. De Bernardin, L. Schiaffino, 'A new water soluble Zn-salophen derivative as a receptor for α-amino-acids: Unexpected chiral discrimination', *Chirality* **2009**, *21*, 104–109.

[19] C. Schmuck, V. Bickert, 'Oxoanion Binding by Flexible Guanidiniocarbonyl Pyrrole–Ammonium Bis-Cations in Water', *J. Org. Chem.* **2007**, *72*, 6832–6839.

[20] E. A. Meyer, R. K. Castellano, F. Diederich, 'Interactions with Aromatic Rings in Chemical and Biological Recognition', *Angew. Chem. Int. Ed.* **2003**, *42*, 1210–1250.

[21] G. Tobajas-Curiel, Q. Sun, J. K. M. Sanders, P. Ballester, C. A. Hunter, 'Substituent effects on aromatic interactions in water', *Chem. Sci.* **2023**, *14*, 6226–6236.

[22] J. Rebek, B. Askew, N. Islam, M. Killoran, D. Nemeth, R. Wolak, 'Synthetic receptors: size and shape recognition within a molecular cleft', *J. Am. Chem. Soc.* **1985**, *107*, 6736–6738.

[23] J. Rebek, D. Nemeth, 'Molecular recognition: three-point binding leads to a selective receptor for aromatic amino acids', *J. Am. Chem. Soc.* **1985**, *107*, 6738–6739.

[24] Y. Kato, M. M. Conn, J. Jr Rebek, 'Water-Soluble Receptors for Cyclic-AMP and Their Use for Evaluating Phosphate-Guanidinium Interactions', *J. Am. Chem. Soc.* **1994**, *116*, 3279–3284.

[25] J. Rebek, L. Marshall, R. Wolak, K. Parris, M. Killoran, B. Askew, D. Nemeth, N. Islam, 'Convergent functional groups: synthetic and structural studies', *J. Am. Chem. Soc.* **1985**, *107*, 7476–7481.

[26] J. Rebek, B. Askew, M. Killoran, D. Nemeth, F. T. Lin, 'Convergent functional groups. 3. A molecular cleft recognizes substrates of complementary size, shape, and functionality', *J. Am. Chem. Soc.* **1987**, *109*, 2426–2431.

[27] P. Thordarson, 'Determining association constants from titration experiments in supramolecular chemistry', *Chem. Soc. Rev.* **2011**, *40*, 1305–1323.
[28] J. Rebek, B. Askew, P. Ballester, A. Costero, 'Convergent functional groups. 5. Ternary complexes in the molecular recognition of .beta.-arylethylamines', *J. Am. Chem. Soc.* **1988**, *110*, 923–927.
[29] T. Wiseman, S. Williston, J. F. Brandts, L.-N. Lin, 'Rapid measurement of binding constants and heats of binding using a new titration calorimeter', *Anal. Biochem.* **1989**, *179*, 131–137.
[30] J. Tellinghuisen, 'Isothermal titration calorimetry at very low c', *Anal. Biochem.* **2008**, *373*, 395–397.
[31] S. B. Ferguson, E. M. Seward, F. Diederich, E. M. Sanford, A. Chou, P. Inocencio-Szweda, C. B. Knobler, 'Strong enthalpically driven complexation of neutral benzene guests in aqueous solution', *J. Org. Chem.* **1988**, *53*, 5593–5595.
[32] W. B. Turnbull, A. H. Daranas, 'On the Value of *c*: Can Low Affinity Systems Be Studied by Isothermal Titration Calorimetry?', *J. Am. Chem. Soc.* **2003**, *125*, 14859–14866.

Received November 29, 2023
Accepted January 10, 2024